Journal of Zoology

Journal of Zoology. Print ISSN 0952-8369

Geometric morphometrics shows differences and similarities in skull shape between the red and giant pandas

B. Figueirido[1,2], F. J. Serrano-Alarcón[1] & P. Palmqvist[1]

1 Área de Paleontología, Departamento de Ecología y Geología, Facultad de Ciencias, Campus Universitario de Teatinos, Málaga, Spain
2 Department of Ecology and Evolutionary Biology, Division of Biology and Medicine, Box G-B206, Brown University, Providence, RI 02912, USA

Keywords
convergent evolution; skull morphology; landmark-based morphometrics; biomechanical constraints; *Ailuropoda melanoleuca*; *Aiulurus fulgens*.

Correspondence
Paul Palmqvist, Área de Paleontología, Departamento de Ecología y Geología, Facultad de Ciencias, Campus Universitario de Teatinos, 29071 Málaga, Spain.
Email: ppb@uma.es

Editor: Andrew Kitchener

Received 27 July 2011; revised 22 October 2011; accepted 27 October 2011

doi:10.1111/j.1469-7998.2011.00879.x

Abstract

A morphometric analysis of the skull of the red or lesser panda, *Aiulurus fulgens* (Ailuridae), and the giant panda, *Ailuropoda melanoleuca* (Ursidae), was performed for evaluating the importance of natural selection and phylogenetic constraints in shaping the convergent morphological adaptations of these peculiar carnivores for feeding on bamboo. Principal components and discriminant analyses of landmark data was used in a comparative study across the families Procyonidae, Ursidae and Ailuridae. Skull morphospaces show that major patterns of morphological variation among these arctoid carnivorans correlate with differences in their feeding behavior. More specifically, this study has shown an extreme convergence in skull shape between the two bamboo specialists. Following the most recent molecular and morphological phylogenies, as well as the poor evidence from the fossil record, it seems highly improbable that homology could explain the shared morphology of the giant and red pandas, which lineages diverged ~40 million years ago. On the contrary, most phylogenetic and paleontological data suggest that convergent or parallel evolution (homoplasy) would be the evolutionary process shaping the common morphological traits of these unusual carnivorans. Therefore, the overall resemblance in skull shape between the giant and red pandas was probably driven by extrinsic factors (natural selection and adaptation for feeding on bamboo) as well as by intrinsic ones (the shared developmental pathway of the carnivoran skull, which posed some biomechanical constraints on the direction of the evolution of pandas).

Introduction

Few organisms have received as much attention from an evolutionary point of view as the living pandas, which are often cited as an example of extreme evolutionary convergence (Bardenfleth, 1913; Raven, 1936; Davis, 1964; Chorn & Hoffmann, 1978; Gould, 1978; Roberts & Gittleman, 1984; Schaller *et al*., 1989; Schaller, 1993; Gittleman, 1994; Pradhan, Saha & Khan, 2001; Antón *et al*., 2006; Salesa *et al*., 2006*a*,*b*; Sims *et al*., 2007; Zhang *et al*., 2007). These emblematical mammals belong to two species from separate families, the giant panda (*Ailuropoda melanoleuca*, Ursidae) and the red or lesser panda (*Ailurus fulgens*, Ailuridae). Both are native to Central Asia, exhibit a highly specialized anatomy and have an unusual trophic behavior among the order Carnivora, as they feed almost entirely on bamboo.

The morphological convergence between the pandas includes a number of features that represent adaptations for the oral processing of tough plants, for example the presence of broad premolar and molar teeth, large zygomatic arches, a wide temporal fossa and a powerful jaw with a well-developed masseteric fossa and an extremely large coronoid process. The enlarged masseter muscles and cheek teeth of pandas are well suited to crushing and chewing bamboo (Chorn & Hoffmann, 1978; Figueirido *et al*., 2010, 2011*a*). In fact, a comparative study of bite force in carnivorans showed that the red and giant pandas have some of the highest bite forces for their body size (Christiansen & Wroe, 2007). Given that an in-depth mastication increases the availability of plant cell contents and increases also particle surface area, this allows better digestion of food, which is crucial for pandas given their low-quality diet and the limitations posed by their carnivoran gut. In addition, both pandas have an enlarged wrist bone, the radial sesamoid, which functions as an opposable 'thumb' and is used for manipulating bamboo stems (Endo *et al*., 1996, 1999, 2001*a*,*b*, 2008; but see Salesa *et al*., 2006a).

From a nutritional point of view, bamboo is composed primarily of structural carbohydrates (cellulose, hemicellulose and lignin), as the majority of the plant is made of the central stalk and branches. The high indigestibility of these compo-

nents poses a challenge for pandas because they have limited ability to digest structural carbohydrates given their gastrointestinal tract, typical of a carnivore, with very limited capacity for extensive microbial digestion (Dierenfeld *et al*., 1982; Sims *et al*., 2007). In addition, the giant panda is an exception among the living bears in that it has a comparatively short small intestine and a very rapid passage time of ingesta (from only 5 to 11 h; Edwards *et al*., 2006). These features contribute to less-complete digestion, which forces the giant panda to consume large amounts of bamboo (up to 12 kg per day) to meet its daily energy requirements (Li, 1986). However, it is worth noting that although previous attempts for finding cellulose-digesting symbionts in pandas have failed, a recent study of giant pandas' fecal samples has shown seven taxonomically distinct entities closely related to *Clostridium* that are able to digest cellulose (Zhu *et al*., 2011).

Compared to other meat-eating carnivores with high-protein intakes, both pandas differ in a number of life-history traits, including a reduced birth weight, a slow growth rate and, specially, a low basal metabolic rate. This may relate to their low-quality diet, but may also evidence their low level of physical activity (Gittleman, 1994).

Given their peculiar diet and shared morphological specializations, the systematic position and phylogenetic relationships of pandas have been under debate for over a century. For example, several authors grouped them within the same clade, either in Procyonidae (e.g. Mivart, 1885; Lankester & Lydeker, 1901; Gregory, 1936; Simpson, 1945) or in Ursidae (e.g. Segall, 1943; Ginsburg, 1982). However, new approaches for reconstructing phylogenies that combine molecular data with morphologically based inferences have shown that both species diverged during the early Oligocene and belong to different families within the suborder Caniformia: Ailuridae for the red panda and Ursidae for the giant panda (Goldman, Giri & O'Brien, 1989; Ledje & Arnason, 1996; Flynn & Nedbal, 1998; Bininda-Emonds, Gittleman & Purvis, 1999; Ginsburg, 1999; Flynn *et al*., 2000, 2005). However, although the phylogenetic position of *Ailuropoda* as a sister lineage to all living ursids is well documented (Davis, 1964; Flynn, Neff & Tedford, 1988; Wyss & Flynn, 1993), the evolutionary affinities of *Ailurus* have yet to be resolved: while some authors suggest a close phylogenetic relationship with Ursidae (e.g. Segall, 1943; Hunt, 1974; Ginsburg, 1982; Wozencraft, 1989), others favor Procyonidae (e.g. Flower & Lydekker, 1891; Beddard, 1902; Tagle *et al*., 1986; Goldman *et al*., 1989; Wayne *et al*., 1989; Bininda-Emonds *et al*., 1999) or even Mephitidae (Flynn *et al*., 2000, 2005; Delisle & Strobeck, 2005). In any case, the status of *Ailurus* and *Ailuropoda* as distantly related taxa makes their shared morphology, particularly the presence of a false extra 'thumb', one of the most remarkable examples of evolutionary convergence among mammals (e.g. Bardenfleth, 1913; Raven, 1936; Davis, 1964; Gould, 1978; Salesa *et al*., 2006*b*; Zhang *et al*., 2007).

Convergence and parallelism are both central issues in evolutionary theory (Wroe & Milne, 2007) and the study of mammalian evolution has provided key evidence for understanding them (Madsen *et al*., 2001; Nevo, 2001; de Winter & Oxnard, 2001; Figueirido *et al*., 2011*b*; Goswami, Milne & Wroe, 2011). However, few comparative analyses have addressed the common adaptations of pandas from a functional perspective, in spite of the fact that only such studies could shed light on the origin of the extreme morphophysiological convergence between these peculiar carnivorans. For example, it is worth noting that Davis (1964) drew Thompsonian diagrams of deformed coordinates for exploring the morphological differences between the giant panda and the other bears. However, this study was hampered by the lack of technological advances for obtaining mathematical shape descriptors currently available. As a result, Davis (1964) could not develop a multivariate approach based on geometric morphometrics for characterizing the patterns of shape change in arctoid carnivorans.

More recently, Zhang *et al*. (2007) performed an analysis of mandibular morphology in the giant panda and compared it to other sympatric Chinese carnivores using multivariate approaches. However, they did not develop a comparative study of skull anatomy between both pandas.

Finally, Figueirido *et al*. (2010) searched among the members of the order Carnivora for patterns of parallel evolution of skull shape toward herbivory, a feeding behavior that represents the opposite extreme of the ancestral carnivorous condition. Apart from the pandas, only three other species have also a diet in which vegetal matter represents at least 90% of their diet, one ursid (the spectacled bear, *Tremarctos ornatus*) and two procyonids (the bushy tailed olingo, *Bassaricyon gabbi* and the kinkajou, *Potos flavus*). This study also used state reconstructions of skull shape for the hypothetical morphology of the ancestral nodes in the phylogenetic tree, which showed a rather limited set of ecomorphological adaptations toward herbivory in the carnivoran skull. Although these adaptations were developed independently in each carnivoran lineage, they were strongly constrained by the phylogenetic legacy of the order Carnivora, which resulted in repeated patterns of biomechanical homoplasy among the members of the three caniform families compared. Specifically, Figueirido *et al*. (2010) showed that, compared to other arctoid carnivorans, the five herbivorous species show a distinct skull shape, including a deep mandibular ramus, a wide coronoid process, a long distance from the jaw condyle to the angular process, a reduced shearing function of the lower carnassial tooth, a brachycephalic cranium with a deep and short snout, anteriorly oriented zygomatic arches and orbits, a short premolar tooth row and enlarged upper molars. In addition, Figueirido *et al*. (2010) showed that, compared to the other three species secondarily adapted to a herbivorous diet, the giant and red pandas have mandibles with a higher coronoid process and a deeper posterior body, enlarged molar tooth rows, more developed zygomatic arches and a shorter, deeper and more stoutly built cranium.

In this study, we have performed a more in-depth morphometric comparison of skull shape between the red and giant pandas using landmark-based methods of geometric morphometrics (Rohlf, 1993; Adams, Rohlf & Slice, 2004; Figueirido, Palmqvist & Pérez-Claros, 2009; Figueirido *et al*., 2010, 2011*a*). Our specific goals are: (1) to quantify the similarities in cranial and jaw anatomy between *Ailurus* and *Ailuropoda* for

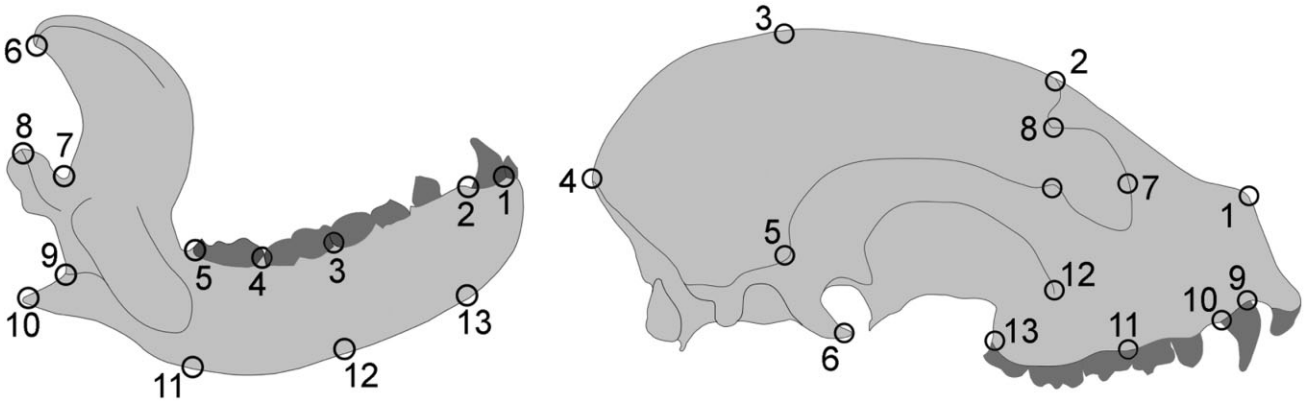

Figure 1 Landmarks used in the morphometric analysis of crania and mandibles, illustrated on a drawing of a red panda skull. Mandible: (1) most antero-dorsal border of the canine alveolus, (2) most postero-dorsal border of the canine alveolus, (3) point between the alveoli of the fourth premolar and the carnassial, (4) point between the alveoli of the first and second molars, (5) posterior edge of the lower tooth row, (6) postero-ventral edge of the coronoid process, (7) intersection between the coronoid and condylar processes, (8) most posterior edge of the articular surface condyle, (9) intersection between the most antero-dorsal point of the angular process and the ascending ramus, (10) tip of angular process, (11) ventral outline below the mesial end of the tooth row, (12) ventral outline below the intersection of the fourth premolar and the carnassial, (13) ventral outline below the most posterior edge of the canine; cranium: (1) most anterior edge of the nasal bones, (2) dorsal outline directly superior to the post-orbital process, (3) dorsal outline directly superior to the end of the zygomatic arch, (4) intersection between the sagittal and nuchal crests, (5) postero-dorsal border of the zygomatic arch, (6) ventral tip of postglenoid process, (7) lacrimal duct, (8) ventral tip of the post-orbital process, (9) most antero-dorsal border of the canine alveolus, (10) most postero-dorsal border of the canine alveolus, (11) point between the alveoli of the third and fourth premolars, (12) ventral intersection between the zygomatic arch and the maxilla, (13) posterior edge of the upper tooth row.

relating them with their similarity in feeding behavior; (2) to explore their anatomical differences in order to clarify the autapomorphies of both species; and (3) to debate on the roles played by evolutionary convergence and historical contingency in shaping the skull of these emblematic mammals.

Table 1 Sample sizes (*n*, crania/mandibles) of the species included in the morphometric analyses. Dietary categories according to the percentage of vegetal matter consumed (H: herbivore, >90%; O: omnivore, 25–90%; F: faunivore, <25%).

Family	Species	*n*	Diet
Ailuridae	*Ailurus fulgens*	(14/12)	H
Ursidae	*Ailuropoda melanoleuca*	(16/12)	H
Ursidae	*Ursus arctos*	(20/30)	O
Ursidae	*Ursus americanus*	(8/9)	O
Ursidae	*Tremarctos ornatus*	(7/8)	H
Ursidae	*Melursus ursinus*	(12/10)	F
Ursidae	*Ursus maritimus*	(10/12)	F
Procyonidae	*Bassaricyon alleni*	(5/4)	O
Procyonidae	*Bassariscus astutus*	(6/5)	O
Procyonidae	*Bassaricyon gabbi*	(3/3)	H
Procyonidae	*Bassaricyon sumichastri*	(5/5)	O
Procyonidae	*Nasua nasua*	(14/21)	O
Procyonidae	*Nasua narica*	(1/1)	O
Procyonidae	*Potos flavus*	(10/10)	H
Procyonidae	*Procyon cancrovorous*	(7/9)	O
Procyonidae	*Procyon lotor*	(9/7)	O
Mephitidae	*Mephitis mephitis*	(6/4)	O

Materials and methods

This study is based on 153 crania and 160 mandibles belonging to 18 species within Ursidae, Procyonidae, Ailuridae and Mephitidae (Table 1). Only adult specimens were collected for avoiding ontogenetic variation. A total of 26 relocatable landmarks, 13 taken on the mandible and 13 on the cranium, were digitized on high-resolution digital images in direct lateral view (Fig. 1). Their bi-dimensional (x,y) coordinates were obtained using the program TPSdig v.2.11 (Rohlf, 2008). All the specimens were collected at the American Museum of Natural History (New York, USA), the Natural History Museum (London, UK) and the Museum für Naturkunde (Berlin, Germany).

According to the procedure described in Figueirido *et al.* (2009), the specimens were photographed following a protocol designed to minimizing lens distortion and parallax (Marugán-Lobón & Buscalioni, 2004). They were aligned using the generalized least squares Procrustes superimposition method (Bookstein, 1991; Dryden and Mardia, 1998; Adams *et al.*, 2004; Marugán-Lobón & Buscalioni, 2006) for both samples (i.e. mandibles and crania) separately. Principal component analyses (PCAs) were computed separately from the covariance matrices of the aligned coordinates of cranial and mandibular shape, respectively, using all the specimens included in the sample. Discriminant analyses (DAs) were also computed separately from the Procrustes coordinates of cranial and mandibular shape for identifying skull shape similarities between both pandas and their differences with other related arctoid carnivorans (i.e. procyonids, mephitids and

ursids). A permutation test for the Procrustes and Mahalanobis distances between both mean shapes was used for computing the statistical significance of the discrimination between the groups compared (Klingenberg *et al*., 2012).

Skull shape differences between *Ailurus* and *Ailuropoda* were reported with a second round of PCAs from the covariance matrices of aligned coordinates for cranial and mandibular shape using only the specimens from both species of pandas. In addition, a second round of DAs was computed separately from the aligned coordinates of cranial and mandibular shape for discriminating skull shape between *Ailurus* and *Ailuropoda*. As before, the statistical significance of the discrimination was computed from a permutation test for the Procrustes and Mahalanobis distances between both mean shapes (Klingenberg *et al*., 2012).

All the geometric morphometric procedures and statistical analyses were carried out with MORPHOJ software package (Klingenberg, 2011).

Results

Skull shape similarities

The PCA of the aligned coordinates for the 26 landmarks describing jaw and cranial shape yielded 22 PCs (Supporting Information Table S1, Fig. S1). The regression analysis between the specimens' centroid size (Cs) and their scores on the third PC derived from jaw shape was significant ($P < 0.0001$). Similarly, the regression between Cs values and the scores in the second PC computed from cranial shape was also significant ($P < 0.0001$). This means that the patterns of morphological variation described by these axes result from allometric effects (Fig. S2). For this reason, we only show the results of the first two PCs in the case of the mandible and of the first and third PCs in the case of the cranium, as they contain the most relevant information regarding shape change among the specimens studied.

Figure 2a shows the morphospace depicted from the first two PCs derived from mandibular morphology, which jointly account for nearly 56% of the original variance in landmark positions. The first PC explains the gradient of shape change between the jaws of the red panda (*A. fulgens*), the giant panda (*A. melanoleuca*) and the frugivorous kinkajou (*Potos flavus*), which all take negative scores, to the jaws of other procyonids, ursids and mephitids, which tend to score more positively (Fig. 2a, *x*-axis). The second PC mainly separates the kinkajou jaws, which all take positive scores, from those of pandas (Fig. 2a, *y*-axis).

Figure 2b shows the morphospace depicted from the first and third PCs derived from cranial analysis, which jointly explain more than 57% of the original variance in landmark displacements. The first PC describes the shape changes that take place from the crania of the red panda and the kinkajou, both with negative scores, to the crania of the other arctoid carnivores included in the sample, of which half approximately score positively (Fig. 2b; *x*-axis). The third PC mainly separates the crania of giant pandas, which all take positive scores, from those of other arctoid carnivorans, most of which take negative scores on this axis (Fig. 2b, *y*-axis).

Figure 2c,d show the transformation grids from the consensus configuration of landmarks that help to visualize the morphological variation along the two axes of the jaw and cranial morphospaces, respectively.

After visual inspection of these results, we can conclude that it is the combination of the first and second PCs derived from jaw analysis, which defines the mandibles of *Ailurus* and *Ailuropoda* into a limited region of the mandible morphospace (Fig. 2a). In contrast, both pandas do not converge on the same place of the cranial shape space, although they tend to scatter on the upper left corner of this graph (Fig. 2b).

These results suggest that the giant and red pandas have a unique combination of mandibular and cranial traits among the arctoid carnivorans included in the analyses. However, this is particularly evident in the case of the mandible, which seems to be less morphologically constrained than the cranium (Figueirido *et al*., 2009, 2010, 2011*b*). The reason is that while jaw morphology is closely related to food acquisition and processing, the overall cranial anatomy is the result of a compromise between different functions (e.g. feeding, olfactory sense, vision and brain processing). In addition, the mammalian jaw is composed of a single bone, the dentary, while the cranium is made up of 22 bones, eight in the neurocranium and 14 in the splanchnocranium, which results in a higher degree of morphological integration and evolutionary conservatism for the cranium compared to the mandible.

The results obtained with PCA are confirmed by the DAs computed from mandible (Fig. 2e) and cranial (Fig. 2f) shape for discriminating between *Ailurus* plus *Ailuropoda* and the other species. The highly significant discrimination between both groups (100% of correct reclassifications) allows recognizing a set of skull traits shared by the two pandas, which allows differentiating them from other arctoid carnivorans. Therefore, the mandibles of *Ailurus* and *Ailuropoda* are comparatively deeper and more concave, with a taller and narrower coronoid process, a more robust articular condyle, an angular process more distantly positioned from the jaw condyle and larger cheek teeth (Fig. 2e). Similarly, the crania of the red and giant pandas are brachycephalic, showing a short snout, a highly vaulted calvarium, a short braincase, broad zygomatic arches, a well-developed postglenoid process, large molars and comparatively small canines (Fig. 2f).

Skull shape differences

The PCA of the aligned coordinates for the 26 landmarks that describe jaw and cranial shape of *Ailurus* and *Ailuropoda* yielded 22 PCs (Supporting Information Table S2, Fig. S3).

Figure 3a shows the morphospace depicted from the first two PCs derived from mandibular analysis, which jointly explain more than 75% of the original variance. The first PC describes the shape changes that account for the differences between the mandibles of red pandas, which take negative scores, and those of giant pandas, which score positively (Fig. 3a, *x*-axis). The second PC (Fig. 3a, *y*-axis) explains the

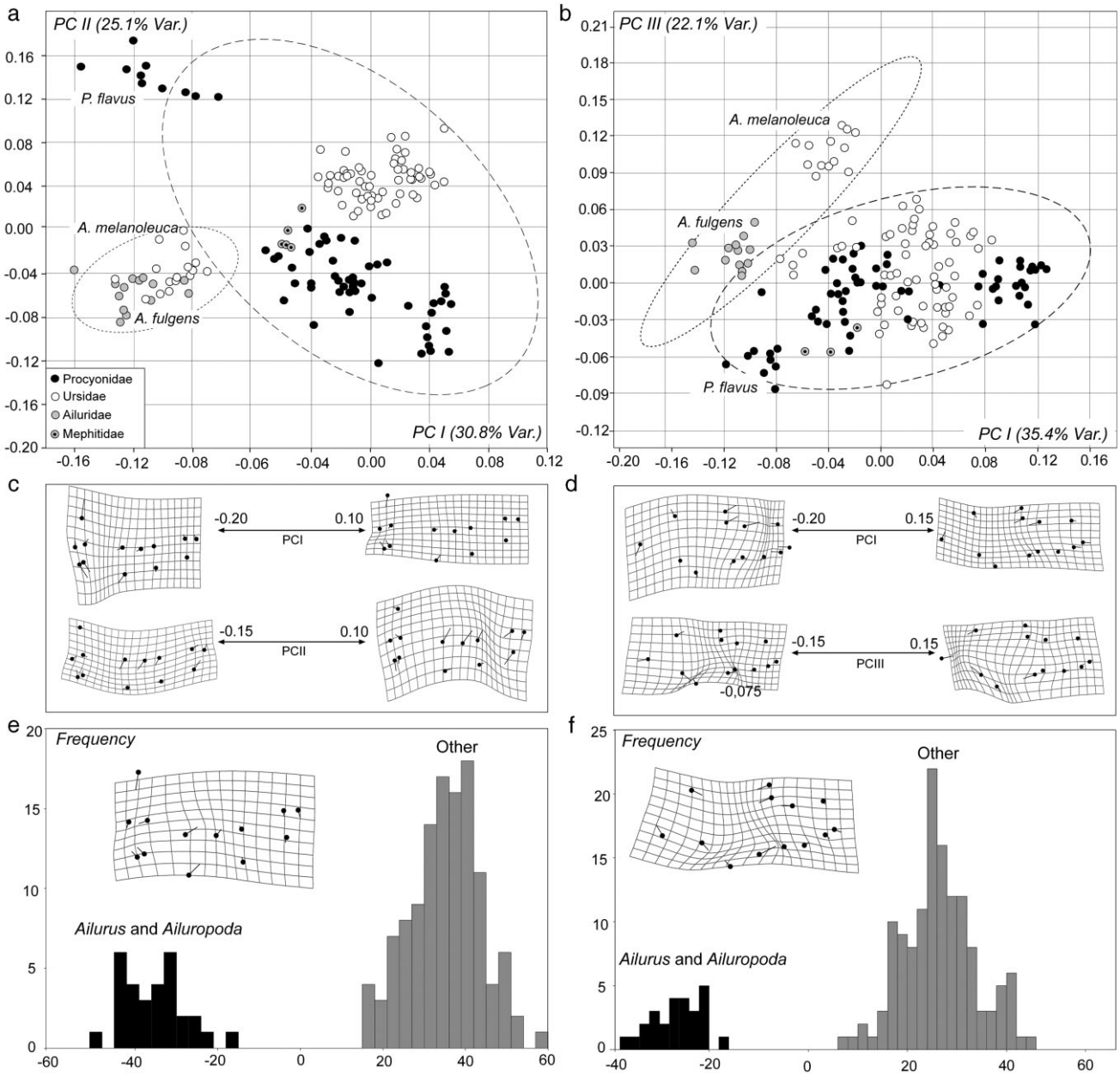

Figure 2 Multivariate analyses that show skull shape similarities between *Ailurus* and *Ailuropoda*. (a) Bivariate plot of the scores derived from PCA of jaw anatomy on the morphospace depicted by the first two PCs. (b) Bivariate plot of the scores derived from PCA of cranial anatomy on the morphospace depicted by the first and third PCs. 95% confidence ellipses are shown in both cases. (c) Morphological variation accounted for by the first two PCs derived from jaw morphology. (d) Morphological variation accounted for by the first and third PCs computed for cranial morphology. In (c) and (d), thin plate splines (TPS) transformation grids show the deformation from the consensus configuration of landmarks to each extreme of the axis. (e) Histogram showing the distribution of the specimens according to their scores on the discriminant function adjusted for jaw morphology. (f) Histogram with the specimens' scores on the discriminant function computed for cranial morphology. The morphological variation accounted for by each discriminant function is shown as a deformation grid of the change in the consensus configuration of landmarks from *Ailurus* and *Ailuropoda* to the other arctoid carnivorans.

intraspecific variation within each species. Figure 3c shows the morphological gradients described by these axes.

Figure 3b shows the morphospace depicted form the first two PCs derived from cranial analysis. As in the case of the mandible, the first PC relates mainly to the shape changes between the crania of the red pandas, which take negative scores, to those of giant pandas, which score positively (Fig. 3b; *x*-axis). The second PC (Fig. 3b, *y*-axis) explains

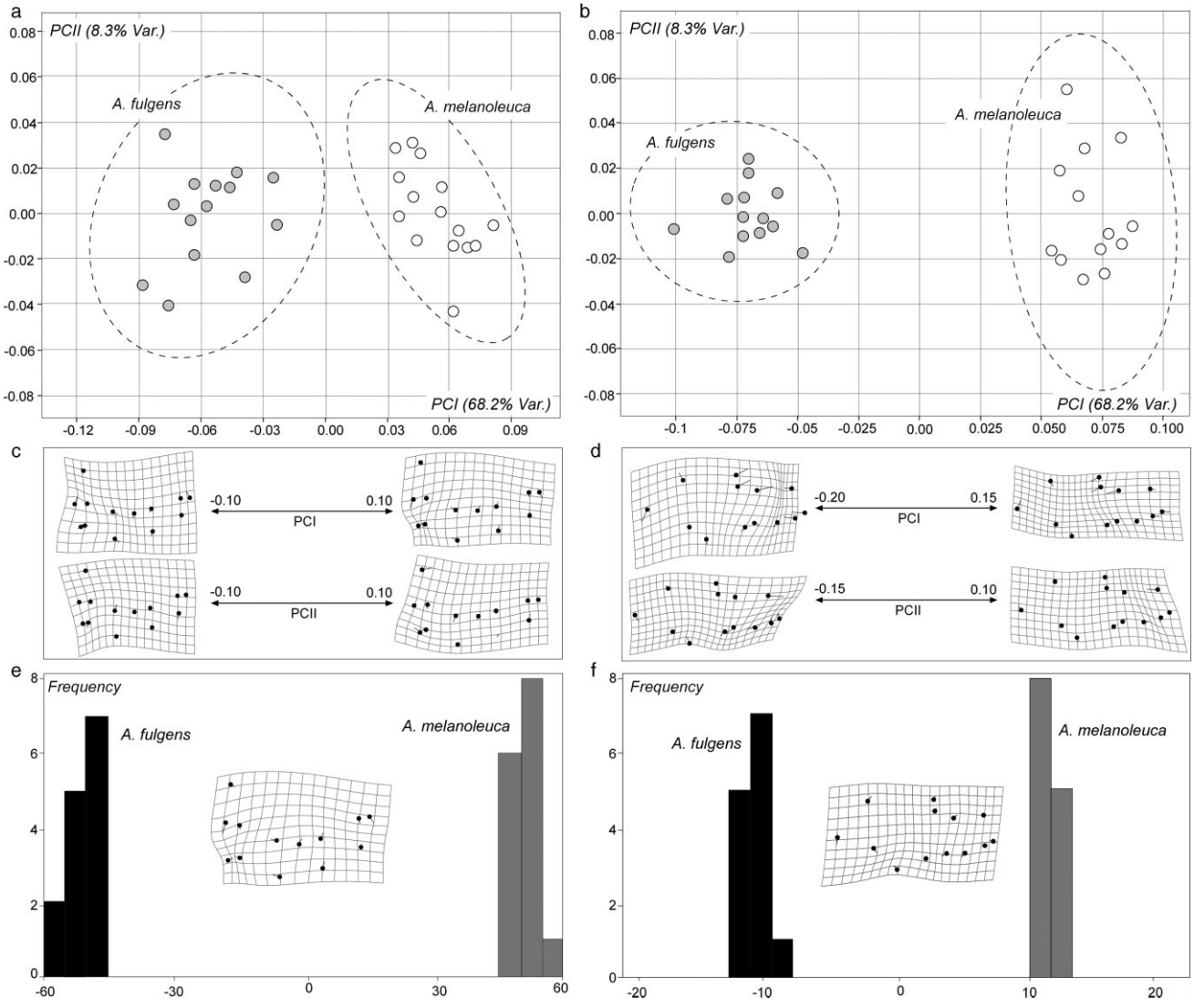

Figure 3 Multivariate analyses that show skull shape differences between *Ailurus* and *Ailuropoda*. (a) Bivariate plot of the scores derived from PCA of jaw anatomy on the morphospace depicted by the first two PCs. (b) Bivariate plot of the scores derived from PCA of cranial anatomy on the morphospace depicted by PCI and PCII. 95% confidence ellipses are shown in both cases. (c) Morphological variation accounted for by the first two PCs derived from jaw morphology. (d) Morphological variation accounted by the first and third PCs computed for cranial morphology. In (c) and (d), TPS transformation grids show the deformation from the consensus configuration of landmarks to each extreme of the axis. (e) Histogram showing the distribution of the specimens according to their scores on the discriminant function adjusted for jaw morphology. (f) Histogram with the scores of the specimens on the discriminant function computed for jaw morphology. The morphological variation accounted for by each discriminant function is shown as a deformation grid of the change in the consensus configuration of landmarks from the red panda to the giant panda.

again the changes resulting from intraspecific variation in both species. Figure 3d describes the traits associated to these morphological gradients. However, given the fact that only two species were analyzed and that they have quite different body masses (~5 kg for *A. fulgens* and ~100 kg for *A. melanoleuca*; Chorn & Hoffmann, 1978; Roberts & Gittleman, 1984), it is not possible to evaluate if the shape changes reported in the mandible and the cranium result from size differences (i.e. interspecific allometry).

DAs between both pandas for mandible (Fig. 3e) and cranial (Fig. 3f) anatomy also show a very significant discrimination (100% of correct reclassifications). However, the small sample sizes of the two species and the high dimensionality of the data imply that the power of the significance test could be low. In spite of that, it is worth noting that all the specimens were correctly classified using the leave-one-out method for cross validation. In addition, the morphological traits of the jaw and cranium that allow discriminating between both

species are those that contribute more to the first PCs obtained from mandible and cranial analyses, respectively. As a result, compared to the mandible of the giant panda, the red panda has a shallower mandibular body, a shorter molar tooth row (which reflects the absence of the third lower molar in this species), a longer but less vertically oriented coronoid process, a more developed angular process and a shorter distance between the condylar and angular processes (Fig. 3e). The cranium is also deeper in the red panda than in the giant panda, has less developed zygomatic arches and a reduced glenoid fossa, a larger braincase and a shorter molar tooth row (Fig. 3f). Some of these features probably reflect the effects of allometric growth (e.g. braincase length scales with negative allometry in carnivorans; Radinsky, 1984).

Discussion

The results obtained show that the two pandas, *A. melanoleuca* and *A. fulgens*, share a number of craniodental traits that may be interpreted as common adaptations toward bamboo feeding. Such morphological convergence, which is particularly evident in the case of the mandible, opens the possibility of hypothesizing on the evolutionary causes below the shared morphology of these arctoid carnivores.

There are two possible evolutionary scenarios that could explain the common morphological patterns related to the dietary preferences of pandas. The first is that these traits were already present in their most immediate common ancestor (homology), which would obviously imply that both pandas should be grouped within the same clade. This could be the case if the red panda was closely related to Ursidae. However, most molecular and morphological phylogenies indicate that *A. fulgens* is more closely related to Procyonidae or Mephitidae, as discussed above. In addition, the scarce fossil record of *Ailurus* and *Ailuropoda* points in the same direction: there is consistent evidence that the common ancestor of Ailuridae was a generalized omnivore, not a bamboo feeder, which indicates that the highly specialized morphology of *Ailurus* is secondary (Salesa *et al*., 2006*b*). The craniodental adaptations of *Ailuropoda* for a durophagous diet based on bamboo were already evident in the late Pliocene species *A. microta* (Figueirido *et al*., 2011*a*; Jin *et al.*, 2007), although dental and basicranial anatomy indicate a less-specialized morphology in the early history of the giant panda lineage (McLellan & Reiner, 1994; Jin *et al*., 2007).

Given that homology is an improbable cause for explaining the evolution of the shared traits of giant and red pandas, how can we explain their extreme morphological and ecological resemblance? We hypothesize here that similar selection pressures posed by similar ecological requirements (i.e. bamboo feeding) drove morphological evolution and feeding specialization in the unrelated *Ailuropoda* and *Ailurus*. Thus, the processes that more likely gave rise to the common traits of pandas would be either convergent or parallel evolution (homoplasy, as shown by Figueirido *et al.* (2010)). The independent evolution of similar skull morphologies could have resulted from a common developmental basis or genetic channeling, which would indicate that parallel evolution played a major role in the evolution of pandas. In contrast, if the morphological traits shared by both lineages of pandas evolved from different ancestral features (and thus through different developmental pathways), convergent evolution would be then the main process responsible of shaping these common traits (Brakefield, 2006). It is well documented that closely related taxa often use different developmental pathways to reach the same phenotype and vice versa (Arendt & Reznick, 2008), at least within vertebrates (Leander, 2008). For these reasons, distinguishing parallel from convergent evolution is a rather difficult task (Arendt & Reznick, 2008). In addition, many authors cast doubts on whether there is a clear-cut theoretical distinction between these two evolutionary processes, which are frequently envisaged as the extremes of a continuum (Meyer, 1999; Gould, 2002; Desutter-Grandcolas *et al*., 2005; Hall, 2007; Abouheif, 2008; Arendt & Reznick, 2008).

In summary, the question is, could natural selection have favored other morphological designs highly specialized for bamboo feeding different to those shown by pandas? Or, on the contrary, is the panda's morphology the only possible given the underlying developmental channels and shared genetic basis inherited from their last common carnivoran ancestor ~40 million years ago? The answers to these questions demand combined morphometric studies based on phylogenetic reconstructions, which are key points for providing a better understanding of the evolutionary history of pandas.

Acknowledgments

This work was supported by Research Projects CGL2006-13808-C02-02 and CGL2008-04896, funded by the Spanish Ministry of Science and Innovation, and Fulbright Postdoctoral Grant in the University of Brown (Rhode Island, USA) to B. Figueirido. We gratefully acknowledge the insightful comments from two anonymous reviewers.

References

Abouheif, E. (2008). Parallelism as the pattern and process of mesoevolution. *Evol. Dev.* **10**, 3–5.

Adams, D.C., Rohlf, F.J. & Slice, D. (2004). Geometric morphometrics: ten years of progress following the 'revolution'. *Ital. J. Zool.* **71**, 5–16.

Antón, M., Salesa, M.J., Pastor, J.F., Peigné, S. & Morales, J. (2006). Implications of the functional anatomy of the hand and forearm of *Ailurus fulgens* (Carnivora, Ailuridae) for the evolution of the 'false-thumb' in pandas. *J. Anat.* **209**, 757–764.

Arendt, J. & Reznick, D. (2008). Convergence and parallelism reconsidered: what have we learned about the genetics of adaptation? *Trends Ecol. Evol.* **23**, 26–32.

Bardenfleth, K.S. (1913). On the systematic position of *Aeluropus melanoleucus*. *Mindeskr. Japetus Steenstrup.* **17**, 1–15.

Beddard, F.E. (1902). *Cambridge natural history, 10: Mammalia*. London: Macmillan.

Bininda-Emonds, O.R., Gittleman, J.L. & Purvis, A. (1999). Building large trees by combining phylogenetic information: a complete phylogeny of extant Carnivora (Mammalia). *Biol. Rev.* **74**, 143–175.

Bookstein, F.L. (1991). *Morphometric tools for landmarks data: geometry and biology*. London: Cambridge University Press.

Brakefield, P.M. (2006). Evo-devo and constraints on selection. *Trends Ecol. Evol.* **21**, 362–368.

Chorn, J. & Hoffmann, R.S. (1978). *Ailuropoda melanoleuca*. *Mamm. Spec.* **110**, 1–6.

Christiansen, P. & Wroe, S. (2007). Bite forces and evolutionary adaptations to feeding ecology in carnivores. *Ecology* **88**, 347–358.

Davis, D.D. (1964). The giant panda: a morphological study on evolutionary mechanisms. *Fieldiana, Geol.* **3**, 1–339.

Delisle, I. & Strobeck, C. (2005). A phylogeny of the Caniformia (order Carnivora) based on 12 complete protein-coding mitochondrial genes. *Mol. Phylogenet. Evol.* **37**, 192–201.

Desutter-Grandcolas, L., Lengendre, F., Grandcolas, P., Robillard, T. & Murienne, J. (2005). Convergence and parallelism: is a new life ahead of old concepts? *Cladistics* **21**, 51–61.

Dierenfeld, E.S., Hintz, H.F., Robertson, J.B., Van Soest, P.J. & Oftedal, O.T. (1982). Utilization of bamboo by the giant panda. *J. Nutr.* **112**, 636–641.

Dryden, I.L. & Mardia, K.V. (1998). *Statistical Shape Analysis*. Chichester: John Wiley & Sons.

Edwards, M.S., Zhong, G., Wei, R. & Liu, X. (2006). Nutrition and dietary husbandry. In *Giant pandas: biology, veterinary medicine and management*: 101–158. Wildt, D.E., Zhang, A., Janssen, D.L. & Ellis, S. (Eds). Cambridge: Cambridge University Press.

Endo, H., Hama, N., Niizawa, N., Kimura, J., Itou, T., Koie, H. & Sakai, T. (2008). Three-dimensional imaging of the manipulating apparatus in the lesser panda and the giant panda. In *Anatomical imaging: towards a new morphology*: 61–66. Endo, H. & Frey, R. (Eds). Tokyo: Springer.

Endo, H., Makita, T., Sasaki, M., Arishima, K., Yamamoto, M. & Hayashi, Y. (1999). Comparative anatomy of the radial sesamoid bone in the polar bear (*Ursus maritirnus*), the brown bear (*Ursus arctos*) and the giant panda (*Ailuropoda melanoleuca*). *J. Vet. Med. Sci.* **61**, 903–907.

Endo, H., Sasaki, M., Hayashi, Y., Koie, H., Yamaya, Y. & Kimura, J. (2001a). Carpal bone movements in gripping action of the giant panda (*Ailuropoda melanoleuca*). *J. Anat.* **198**, 243–246.

Endo, H., Sasaki, M., Kogiku, H., Yamamoto, M. & Arishima, K. (2001b). Radial sesamoid bone as a part of the manipulation system in the lesser panda (*Ailurus fulgens*). *Ann. Anat.* **183**, 181–184.

Endo, H., Sasaki, N., Yamagiwa, D., Uetake, Y., Kurohmaru, M. & Hayashi, Y. (1996). Functional anatomy of the radial sesamoid bone in the giant panda (*Ailuropoda melanoleuca*). *J. Anat.* **189**, 587–592.

Figueirido, B., MacLeod, N., Krieger, J., De Renzi, M., Pérez-Claros, J.A. & Palmqvist, P. (2011b). Constraint and adaptation in the evolution of carnivoran skull shape. *Paleobiology* **37**, 490–518.

Figueirido, B., Palmqvist, P. & Pérez-Claros, J.A. (2009). Ecomorphological correlates of craniodental variation in bears and paleobiological implications for extinct taxa: an approach based on geometric morphometrics. *J. Zool. (Lond.)* **277**, 70–80.

Figueirido, B., Palmqvist, P., Pérez-Claros, J.A. & Dong, W. (2011a). Cranial shape transformation in the evolution of the giant panda (*Ailuropoda melanoleuca*). *Naturwissenschaften* **98**, 107–116.

Figueirido, B., Serrano-Alarcón, F.J., Slater, G.J. & Palmqvist, P. (2010). Shape at the cross-roads: homoplasy and history in the evolution of the carnivoran skull towards herbivory. *J. Evol. Biol.* **23**, 2579–2594.

Flower, W.H. & Lydekker, R. (1891). *An introduction to the study of mammals living and extinct*. London: Adam and Charles Black.

Flynn, J.J., Finarelli, J.A., Zehr, S., Hsu, J. & Nedbal, M. (2005). Molecular phylogeny of the Carnivora (Mammalia): assessing the impact of increased sampling on resolving enigmatic relationships. *Syst. Biol.* **54**, 317–337.

Flynn, J.J. & Nedbal, M. (1998). Phylogeny of the Carnivora (Mammalia): congruence vs. incompatibility among multiple data sets. *Mol. Phylogenet. Evol.* **9**, 414–426.

Flynn, J.J., Nedbal, M., Dragoo, J. & Honeycutt, L. (2000). Whence the red panda? *Mol. Phylogenet. Evol.* **17**, 190–199.

Flynn, J.J., Neff, N.A. & Tedford, R.H. (1988). Phylogeny of the Carnivora. In *The phylogeny and classification of the tetrapods. Vol. 2, Mammals*: 73–116. Benton, M. (Ed.). Oxford: Clarendon.

Ginsburg, L. (1982). Sur la position systématique du petit panda, *Ailurus fulgens* (Carnivora, Mammalia). *Geobios (Mem. Spec.)* **6**, 247–258.

Ginsburg, L. (1999). Order Carnivora. In *The Miocene land mammals of Europe*: 109–148. Rössner, G. & Heissig, K. (Eds). Munich: Pfeil.

Gittleman, J.L. (1994). Are the pandas successful specialists or evolutionary failures? *BioScience* **44**, 456–464.

Goldman, D., Giri, P.R. & O'Brien, S.J. (1989). Molecular genetic-distance estimates among the Ursidae as indicated by one- and two-dimensional protein electrophoresis. *Evolution* **43**, 282–295.

Goswami, A., Milne, N. & Wroe, S. (2011). Biting through constraints: cranial morphology, disparity and convergence across living and fossil carnivorous mammals. *Proc. Roy. Soc. B Biol. Sci.* **278**, 1831–1839.

Gould, S.J. (1978). The panda's peculiar thumb. *Nat. Hist.* **87**, 20–30.

Gould, S.J. (2002). *The structure of evolutionary theory*. Cambridge: Harvard University Press.

Gregory, W.K. (1936). On the phylogenetic relationships of the giant panda (*Ailuropoda*) to other arctoid carnivora. *Am. Mus. Novit.* **878**, 1–29.

Hall, B.K. (2007). Homoplasy and homology: dichotomy or continuum? *J. Hum. Evol.* **52**, 473–479.

Hunt, R.M. (1974). The auditory bulla in Carnivora: an anatomical basis for reappraisal of carnivore evolution. *J. Morphol.* **143**, 21–76.

Jin, C., Ciochon, R.L., Dong, W., Hunt, R.M., Liu, J., Jaeger, M. & Zhu, Q. (2007). The first skull of the earliest giant panda. *Proc. Natl. Acad. Sci. U.S.A.* **104**, 10932–10937.

Klingenberg, C.P. (2011). MorphoJ: an integrated software package for geometric morphometrics. *Mol. Ecol. Resour* **11**, 353–357.

Klingenberg, C.P., Duttke, S., Whelan, S. & Kim, M. (2012). Developmental plasticity, morphological variation and evolvability: a multilevel analysis of morphometric integration in the shape of compound leaves. *Journal of Evolutionary Biology* (Online DOI: 10.1111/j.1420-9101.2011.02410.x)

Lankester, E.R. & Lydeker, R. (1901). On the affinities of *Aeluropus melanoleucus*. *Trans. Soc. Lond.* **8**, 163–171.

Leander, B.S. (2008). Different modes of convergent evolution reflects phylogenetic distances: a reply to Arendt and Reznick. *Trends Ecol. Evol.* **23**, 481–482.

Ledje, C. & Arnason, U. (1996). Phylogenetic analyses of complete cytochrome*b* genes of the order Carnivora with particular emphasis on the Caniformia. *J. Mol. Evol.* **42**, 135–144.

Li, Y. (Ed.) (1986). *Morphology of the giant panda: systematic anatomy and organ-histology*. Beijing: Science Press.

Madsen, O., Scally, M., Douady, C.J., Kao, D.J., DeBry, R.W., Adkins, R., Amrine, H.M., Stanhope, M.J., de Jong, W.W. & Springer, M.S. (2001). Parallel adaptive radiations in two major clades of placental mammals. *Nature* **409**, 610–614.

Marugán-Lobón, J. & Buscalioni, A.D. (2004). Geometric morphometrics in macroevolution: morphological diversity of the skull in modern avian form in contrast to some theropod dinosaurs. In *Morphometrics: applications in biology and paleontology*: 157–171. Elewa, A.M.T. (Ed.). New York: Springer.

Marugán-Lobón, J. & Buscalioni, A.D. (2006). Avian skull morphological evolution: exploring exo- and endocranial covariation with two-block partial least squares. *Zoology* **109**, 217–230.

McLellan, B. & Reiner, D.C. (1994). A review of bear evolution. *Int. Conf. Bear Res. Manage.* **9**, 85–96.

Meyer, A. (1999). Homology and homoplasy: the retention of genetic programmes. In *homology*: 141–157. Bock, G. (Ed.). Chichester: Wiley & Son.

Mivart, G. (1885). On the anatomy, classification, and distribution of the Arctoidea. *Proc. Zool. Soc. Lond.* **1885**, 340–404.

Nevo, E. (2001). Evolution of genome–phenome diversity under environmental stress. *Proc. N.Y. Acad. Sci.* **98**, 623–6240.

Pradhan, S., Saha, G.K. & Khan, J.A. (2001). Ecology of the red panda *Ailurus fulgens* in the Singhalila National Park, Darjeeling, India. *Biol. Conserv.* **98**, 11–18.

Radinsky, L.A. (1984). Basicranial axis length v. skull length in analysis of carnivore skull shape. *Biol. J. Linn. Soc.* **22**, 31–41.

Raven, H.C. (1936). Notes on the anatomy on the viscera of the giant panda (*Ailuropoda melanoleuca*). *Am. Mus. Novit.* **877**, 1–223.

Roberts, M.S. & Gittleman, J.L. (1984). *Ailurus fulgens*. *Mamm. Spec.* **222**, 1–8.

Rohlf, F.J. (2008). *TpsDig, ver. 2.11*. Digitize landmarks and outlines. Department of Ecology and Evolution, State University of New York at Stony Brook [computer program and documentation].

Salesa, M.J., Antón, M., Peigné, S. & Morales, J. (2006b). Evidence of a false thumb in a fossil carnivore clarifies the evolution of pandas. *Proc. Natl. Acad. Sci. U.S.A.* **109**, 379–382.

Salesa, M.J., Siliceo, G., Antón, M., Abella, J., Montoya, P. & Morales, J. (2006a). Anatomy of the 'false thumb' of *Tremarctos ornatus* (Carnivora, Ursidae, Tremarctinae): phylogenetic and functional implications. *Estud. Geol.* **62**, 389–394.

Schaller, G.B. (1993). *The last panda*. Chicago: University of Chicago Press.

Schaller, G.B., Qitao, T., Johnson, K.G., Wang, X., Shen, H. & Hu, J. (1989). The feeding ecology of giant pandas and Asiatic black bears in the Tangjiahe Reserve, China. In *Carnivore behaviour, ecology, and evolution*, Vol. **1**: 212–241. Gittleman, J.L. (Ed.). Ithaca: Cornell University Press.

Segall, W. (1943). The auditory region of the arctoid carnivores. *Fieldiana, Zool.* **29**, 33–59.

Simpson, G.G. (1945). The principles of classification and classification of mammals. *Bull. Am. Mus. Nat. Hist.* **85**, 1–350.

Sims, J.A., Parsons, J.L., Bissell, H.A., Ouellette, J.R. & Rude, B.J. (2007). Determination of bamboo-diet digestibility and fecal output by giant pandas. *Ursus* **18**, 38–45.

Tagle, D.A., Miyamoto, M.M., Goodman, M., Hofmann, O., Braunitzer, G., Göltenboth, R. & Jalanka, H. (1986). Hemoglobin of pandas: phylogenetic relationships of carnivores as ascertained with protein sequence data. *Naturwissenschaften* **73**, 512–514.

Wayne, R.K., Benveniste, R.E., Janczewski, D.N. & O'Brien, S.J. (1989). Molecular and biochemical evolution of the Carnivora. In *Carnivore behaviour, ecology, and evolution*, Vol. **1**: 465–494. Gittleman, J.L. (Ed.). Ithaca: Cornell University Press.

de Winter, W. & Oxnard, C.E. (2001). Evolutionary radiations and convergences in the structural organization of mammalian brains. *Nature* **409**, 710–714.

Wozencraft, W.C. (1989). The phylogeny of the recent Carnivora. In *Carnivore behaviour, ecology, and evolution*, Vol. **1**: 495–535. Gittleman, J.L. (Ed.). Ithaca: Cornell University Press.

Wroe, S. & Milne, N. (2007). Convergence and remarkably consistent constraint in the evolution of carnivore skull shape . *Evolution* **61**, 1251–1260.

Wyss, A.R. & Flynn, J.J. (1993). A phylogenetic analysis and definition of the Carnivora. In *Mammal phylogeny: placentals*: 32–52. Szalay, F., Novacek, M. & McKenna, M. (Eds). New York: Springer-Verlag.

Zhang, S., Pan, R., Li, M., Oxnard, C. & Wei, F. (2007). Mandible of the giant panda (*Ailuropoda melanoleuca*) compared with other Chinese carnivores: functional adaptation. *Biol. J. Linn. Soc.* **92**, 449–456.

Zhu, L., Wua, Q., Dai, J., Zhang, S. & Wei, F. (2011). Evidence of cellulose metabolism by the giant panda gut microbiome. *Proc. Natl. Acad. Sci. U.S.A.* (Online DOI:10.1073/pnas.1017956108)

Supporting information

Additional Supporting Information may be found in the online version of this article:

Figure S1 Bivariate plots showing the percentage of variance explained by each principal component derived from mandible (A) and cranial (B) analyses of the sample of arctoid carnivores.

Figure S2 Bivariate plots between the logarithms of centroid size (*x*-axis) and the scores of the specimens on the PCs (*y*-axis). The graphs show the relationship for the first (A), second (B) and third PCs computed for jaw morphology, and for the first (C), second (D) and third (E) PCs derived from cranial morphology.

Figure S3 Bivariate plots showing the percentage of variance explained by each principal component derived from mandible (A) and cranial (B) analyses of *Ailurus* and *Ailuropoda*.

Figure S4 Bivariate plots between the logarithms of centroid size (*x*-axis) and the scores of the specimens in the PCs (*y*-axis). The graphs show the relationship for the first (A) and second (B) PCs computed for jaw morphology, and for the first (C) and second (D) PCs derived from cranial morphology. White circles: *Ailuropoda melanoleuca*, gray circles: *Ailurus fulgens*.

Table S1 Eigenvalues (λ) and percentages of variance explained by the principal components computed in the analysis of skull shape variation in arctoid carnivores.

Table S2 Eigenvalues (λ) and percentages of variance explained by the principal components computed in the analysis of skull shape in the red and giant pandas.

Please note: Wiley-Blackwell are not responsible for the content or functionality of any supporting materials supplied by the authors. Any queries (other than missing material) should be directed to the corresponding author for the article.